

1  
2  
3  
4  
5  
6  
7  
8  
9  
10  
11  
12  
13  
14  
15  
16  
17  
18  
19  
20  
21  
22  
23  
24  
25

The CCCTC-binding factor CTCF represses hepatitis B virus Enhancer I and regulates viral transcription

V D'Arienzo<sup>1^</sup>, J Ferguson<sup>2^</sup>, G Giraud<sup>3</sup>, F Chapus<sup>3</sup>, JM Harris<sup>1</sup>, PAC Wing<sup>1</sup>, A Claydon<sup>2</sup>, S Begum<sup>2</sup>,

X Zhuang<sup>1</sup>, P Balfe<sup>1</sup>, B Testoni<sup>3</sup>, JA McKeating<sup>1\*</sup> and JL Parish<sup>2\*</sup>

<sup>^</sup> Equal contribution

\* shared corresponding authors

1-Nuffield Department of Medicine, University of Oxford, Oxford, UK

2-Institute of Cancer and Genomic sciences, College of Medical and Dental Sciences,

University of Birmingham, UK.

3-CRCL INSERM and Cancer Research Center of Lyon (CRCL), UMR INSERM 1052, Lyon, France.

## 26 ABSTRACT

27 Hepatitis B virus (HBV) infection is of global importance with over 2 billion people exposed to  
28 the virus during their lifetime and at risk of progressive liver disease, cirrhosis and  
29 hepatocellular carcinoma. HBV is a member of the *hepadnaviridae* family that replicates via  
30 episomal copies of a covalently closed circular DNA (cccDNA) genome. The chromatinization of  
31 this small viral genome, with overlapping open reading frames and regulatory elements,  
32 suggests an important role for epigenetic pathways to regulate viral transcription. The  
33 chromatin-organising transcriptional insulator protein CCCTC-binding factor (CTCF) has been  
34 reported to regulate transcription in a diverse range of viruses. We identified two conserved  
35 CTCF binding sites in the HBV genome within Enhancer I and chromatin immunoprecipitation  
36 (ChIP) analysis demonstrated an enrichment of CTCF binding to integrated or episomal copies  
37 of the viral genome. siRNA knockdown of CTCF results in a significant increase in pre-genomic  
38 RNA levels in *de novo* infected HepG2 cells and those supporting episomal HBV DNA  
39 replication. Furthermore, mutation of these sites in HBV DNA minicircles abrogated CTCF  
40 binding and increased pre-genomic RNA levels, providing evidence of a direct role for CTCF in  
41 repressing HBV transcription.

## 42 IMPORTANCE

43 Hepatitis B virus (HBV) is a global cause of liver disease. At least 300 million individuals are  
44 chronically infected with HBV, frequently leading to life-threatening liver cirrhosis and cancer.  
45 Following viral entry, HBV DNA enters the nucleus and is bound by histones that are subject to  
46 epigenetic modification. The HBV genome contains two enhancer elements that stimulate viral  
47 transcription but the interplay between the viral enhancers and promoters is not fully  
48 understood. We have identified the host cell protein CCCTC binding factor (CTCF) as a  
49 repressor of HBV gene expression. CTCF binds to the HBV genome within Enhancer I and  
50 represses transcription of pre-genomic RNA. These findings provide new insights into how HBV  
51 transcription is regulated and show a new role for CTCF as a transcriptional insulator by  
52 associating with the viral genome between Enhancer I and the downstream basal core  
53 promoter.

54

55

## 56 INTRODUCTION

57 Hepatitis B virus (HBV) infection is one of the world's unconquered infections with an estimated  
58 2 billion people exposed to the virus in their lifetime. HBV replicates in hepatocytes and chronic  
59 infection can result in progressive liver disease, cirrhosis and hepatocellular carcinoma (HCC).  
60 HBV is a member of the *hepadnaviridae* family and classified into eight genotypes, A-H, based  
61 on a sequence divergence of greater than 8% (1, 2). Viral genotypes are associated with  
62 differences in clinical outcome and treatment responses (3, 4). The HBV genome is a small,  
63 partially double-stranded relaxed circular DNA (rcDNA) genome of approximately 3.2 Kb.  
64 Following HBV entry into hepatocytes via the liver-specific bile-acid transporter, sodium  
65 taurocholate co-transporting polypeptide (NTCP) (5, 6), rcDNA is released into the nucleus and  
66 is repaired into covalently closed circular DNA (cccDNA). cccDNA persists in the nucleus as  
67 multiple copies of nucleosome-associated minichromosomes which serve as a template for  
68 virus transcription (7). Establishment of the stable long-lived cccDNA intermediate is thought  
69 to be responsible for persistence of HBV infection (8, 9).

70 The HBV genome is transcribed by the host RNA polymerase II (RNA pol II) complex from unique  
71 promoters (basal core promoter (BCP), Sp1, Sp2 and Xp) and transcription start sites (7). This  
72 results in the generation of six major viral RNAs of increasing length with heterogeneous 5'  
73 ends and a common polyadenylation signal (10, 11). The 3.5kb preC transcript encodes pre-  
74 core or e antigen (HBe) protein. Approximately 100 base pairs downstream is the  
75 transcriptional start site for pre-genomic (pg) RNA which encodes the core (HBc) protein and  
76 the viral polymerase (pol). When encapsidated in the cytoplasm, pgRNA forms the template for  
77 the reverse-transcription of new rcDNA molecules by the viral pol (7). The large, medium and  
78 small surface envelope proteins (HBs) are encoded by the 2.4 kb preS1 and 2.1 kb preS2/S  
79 transcripts. The smallest transcript is the 0.7kb X RNA which encodes the hepatitis B virus x  
80 protein (HBx) protein, which has been shown to influence many host cell pathways including  
81 regulation of transcription of viral and host genes, metabolism and cell cycle. Two viral  
82 enhancers play an important role in the regulation of HBV transcription. Enhancer I (EnhI) is  
83 located upstream of and partially overlaps the X promoter (Xp) and regulates transcription of  
84 HBx and core genes. It also directs basal core promoter (BCP) activity (12), which stimulates the  
85 production of both preC and pgRNAs (13). Enhancer II (EnhII) overlaps a large portion of BCP  
86 and functions to stimulate activity of the distal Sp1 and Sp2 promoters as well as Xp and BCP

87 (14). The BCP encodes a negative regulatory element (NRE) that overlaps with Enh II (15) and  
88 has been reported to repress EnhII-mediated promoter activation (16).

89 Nuclear HBV cccDNA is assembled into nucleosomes by cellular histones to form episomal  
90 chromatin (17, 18). The viral DNA is enriched with active epigenetic histone modifications  
91 including trimethylation of lysine 4 (H3K4Me3) and acetylation of lysine 27 on histone 3  
92 (H3K27Ac) but devoid of the repressive marks such as trimethylation of lysine 27 on histone 3  
93 (H3K27Me3) (19, 20). The overlap of active histone marks with RNA pol II occupancy suggests  
94 that viral transcription is regulated by epigenetic modification. In support of this, treating *de*  
95 *novo* infected primary human hepatocytes with inhibitors of the histone acetyltransferase  
96 p300/CBP reduces HBV RNA levels (19). Although the mechanisms underlying the epigenetic  
97 regulation of HBV cccDNA are not fully understood (21), several epigenetic modifiers are  
98 recruited to HBV cccDNA by HBx. As such, HBx behaves as a transcriptional regulator of both  
99 viral and cellular promoters (22) and although HBx cannot bind to DNA directly, it can associate  
100 with components of the basal transcription machinery, transcription factors and transcriptional  
101 co-activators (23). HBx coordinates the recruitment of the CBP/p300 and PCAF histone acetyl  
102 transferases (HAT) to cccDNA while facilitating the exclusion of histone deacetylases (HDACs)  
103 HDAC1 and Sirtuin 1 (Sirt1), resulting in hyperacetylation of cccDNA (24, 25). HBV transcription  
104 is dependent on an array of ubiquitous and liver-specific cellular transcription factors including  
105 the liver specific hepatocyte nuclear factors 1 and 4 (HNF-1/4) and ubiquitously expressed  
106 octamer-binding protein 1 (Oct-1) and specificity protein 1 (SP1) (26).

107 The genomes of metazoans are highly organised into megabase-sized regions termed  
108 topologically-associated domains (TADs) that provide regulatory segmentation required for  
109 appropriate gene expression and replication. TADs are separated by regions enriched in binding  
110 sites of the ubiquitously expressed CCCTC binding factor (CTCF) which stabilises chromatin  
111 loops by anchoring cohesin rings at the base of the loops (27). Such spatial organisation can  
112 create epigenetic boundaries that separate transcriptionally active and inactive chromatin  
113 domains and control cis-regulatory elements such as transcriptional enhancers. CTCF binds to  
114 tens of thousands of either ubiquitous or cell type specific consensus binding sites within the  
115 human genome, regulating both tissue-specific and developmental changes in gene expression  
116 (28).

117 The occupancy of specific CTCF binding sites is dictated by chromatin accessibility and local  
118 epigenetic status (29). In addition to the organisation of chromatin domains, CTCF can function  
119 as a transcriptional repressor or activator by direct association with promoter proximal  
120 elements. CTCF was shown to act as a transcriptional repressor of the *c-myc* oncogene by  
121 creating a roadblock to RNA pol II (30). Conversely, CTCF can physically associate with  
122 transcriptional regulators such as the general transcription factor, TFIID to promote recruitment  
123 of the cyclin dependent kinase 8 (CDK8) resulting in stimulation of RNA pol II activity (31). CTCF  
124 regulates the transcription (up or down) of evolutionarily distinct DNA viruses (32) including:  
125 Kaposi sarcoma-associated herpesvirus; Epstein-Barr virus and herpes simplex virus (33-38).  
126 We have demonstrated that CTCF recruitment to the human papillomavirus (HPV) genome  
127 negatively regulates early promoter usage via host cell differentiation-specific stabilisation of  
128 an epigenetically repressed chromatin loop (39, 40). However, a role in HBV transcription  
129 regulation has not yet been reported, herein we show that CTCF binds HBV DNA and acts as a  
130 repressor of viral transcription.

131

## 132 RESULTS

133 **CTCF binds HBV DNA at conserved sites within enhancer elements.** To assess whether CTCF binds  
134 HBV DNA, we selected two independent 'HBV producer' HepG2 lines, HepG2.2.15 (41) and  
135 HepAD38 (42) that carry integrated copies of 1.3x overlength HBV genomes, maintain cccDNA  
136 and generate infectious virus. We isolated and sheared chromatin from nuclear fractions to  
137 limit contamination of cytoplasmic rcDNA and performed an anti-CTCF chromatin  
138 immunoprecipitation (ChIP) followed by quantitative PCR (ChIP-qPCR). Primers were selected  
139 to amplify 100-200 base pair regions of the HBV genome to provisionally identify CTCF binding  
140 sites. We show low level CTCF binding above the control IgG across the viral DNA with a  
141 significant enrichment in the Xp region in both cell lines (**Fig.1A**). Analysing histone  
142 modifications of HBV chromatin from HepG2.2.15 cells showed the viral DNA lacked the  
143 repressive H3K27Me3, in agreement with previous reports (19, 20) (**Fig.1B**). ChIP for histone  
144 marks associating with active transcription, including H4Ac and H3K4Me3, identified these  
145 epigenetic marks throughout the viral genome, with an enrichment in the BCP and Xp regions.  
146 Since both HepG2.2.15 and HepAD38 cell lines have cccDNA and integrated viral genomes, we  
147 are unable to discriminate CTCF binding between these forms of viral DNA. We therefore

148 studied HepG2 cells expressing an episomal copy of HBV DNA (HepG2-HBV-Epi) (43) to establish  
149 whether CTCF can bind episomal viral DNA. We first assessed whether episomal copies of HBV  
150 DNA are sheared by sonication by PCR amplification of viral targets of increasing length pre-  
151 and post-sonication. While the unsheared chromatin yielded a series of PCR products of  
152 increasing length, only amplicons below 238 base pairs were detected in the sonicated material  
153 (**Fig.1C**). Amplicons over 353 base pairs were barely visible in the sonicated samples,  
154 demonstrating effective shearing of episomal HBV genomes. ChIP of sheared chromatin  
155 isolated from HepG2-HBV-Epi nuclear extracts showed CTCF bound to the EnhI region of the  
156 viral DNA (**Fig.1D**). We noted relatively lower ChIP of viral DNA from the HepG2-HBV-Epi cells  
157 compared to HepG2.2.15 or HepAD38 cells, this may reflect differences in the epigenetic status  
158 of the viral DNA in these model systems. Our observation that CTCF binds to EnhI, the major  
159 transcriptional regulatory element of the BCP and Xp, suggests that CTCF regulates its activity.

160 HepG2.2.15, HepAD38 and HepG2-HBV-Epi cells contain HBV genotype D and having  
161 demonstrated that CTCF associates with viral DNA in all three cell lines, we used an open access  
162 CTCF binding site database (<http://insulatordb.uthsc.edu/>) to identify putative CTCF binding  
163 sites within HBV genotype D. We identified two CTCF binding sites (BS) between nucleotides  
164 1194-1209 in EnhI (CTCF BS1) and 1275-1291 in the Xp (CTCF BS2), consistent with the single  
165 binding peak observed in our ChIP-qPCR analysis. Importantly, these binding sites are  
166 conserved amongst all HBV genotypes (>7000 sequences in HBV database [HBVdb.fr]) (**Fig.2A**).  
167 The *hepadnaviridae* family includes a number of related viruses that infect other species  
168 including birds, mammals, fish, reptiles and amphibia. Inspection of reference sequences from  
169 distinct *hepadnaviridae* showed that both consensus CTCF binding sites are conserved in  
170 viruses infecting primates and the majority of mammals and bats but are absent from viruses  
171 infecting birds, fish or amphibia, demonstrating evolutionary conservation of both CTCF binding  
172 sites (**Fig.2B**).

173 **CTCF represses HBV Enhancer I.** To analyse the role of CTCF in regulating HBV enhancer activity,  
174 we used promoter constructs that encode Firefly luciferase under the control of the BCP (nt  
175 900-1859) or EnhI and Xp (nt 900-1358) (**Fig.3A**) (44). We noted that the BCP showed a  
176 significantly lower (4-fold) activity compared to the EnhI construct, most likely reflecting the  
177 presence of a NRE at nt1613-1636 that can repress BCP activity (**Fig.3B**). To analyse the function  
178 of CTCF in regulating EnhI activity, we silenced CTCF in HepG2-NTCP using an siRNA Smartpool

179 (Fig.3C), transfected the viral promoter plasmids along with a *Renilla* luciferase control plasmid  
180 and measured activity after 72h. Knockdown of CTCF protein increased Enh1 activity, however  
181 we noted a minimal effect on the BCP activity, suggesting that CTCF represses Enh1 but this  
182 effect is limited in the presence of an NRE in the full transcriptional reporter construct (Fig.3D).  
183 To assess whether the putative CTCF BS mediated the control of Enh1, we introduced silent  
184 mutations into the pEnh1-Luc designed to abrogate CTCF binding (45), without altering the  
185 polymerase protein sequence as this would adversely affect subsequent experiments with  
186 intact HBV genomes (Fig.3A). Mutation of either CTCF BS1 (BS1m) or BS2 (BS2m) in isolation or  
187 in combination (BS1/2m) abrogated the increase in Enh1 activity following CTCF depletion  
188 (Fig.3E). Together, these data suggest that CTCF binds to both motifs within Enh1 to repress its  
189 activity.

190 **Silencing CTCF increases HBV preC/pgRNA levels.** To determine the effect of CTCF depletion on  
191 viral transcripts we selected to use the HepG2-HBV-Epi cells as we previously demonstrated  
192 CTCF binding to the viral genome. We confirmed effective knock-down of CTCF at the protein  
193 and RNA level 72h post-siRNA transfection (Fig.4A and B). We measured HBV RNAs by RT-qPCR  
194 as previously described (46) and observed a significant increase in preC/pgRNA levels following  
195 CTCF depletion (Fig.4C) and an overall increase in total HBV transcripts following CTCF depletion  
196 (Fig.4D). To determine whether the observed increase in preC/pgRNA levels was due to an  
197 alteration of the HBV epigenome following CTCF depletion we measured H4Ac modification of  
198 viral DNA as this was previously reported to associate with HBV transcription (47). Silencing of  
199 CTCF in HepG2-HBV-Epi cells increased H4Ac abundance within the viral enhancers, BCP Xp and  
200 BCP, suggesting that CTCF regulates the epigenetic status of HBV cccDNA (Fig.4E).

201 Hepatocytes are non-proliferating in the healthy liver and most reports studying HBV infection  
202 *in vitro* use dimethyl sulfoxide (DMSO) to arrest cells (48). As DMSO has pleiotropic effects on  
203 host gene expression (49, 50) we were interested to assess the effects of DMSO on CTCF  
204 expression. We noted a significant reduction in CTCF protein levels in DMSO treated cells (Sup  
205 Fig.S1). We therefore studied the role of CTCF in HBV transcription in non-DMSO treated  
206 HepG2-NTCP cells where our protein of interest is abundant.

207 To extend our studies and to validate a role for CTCF to repress viral transcription during a *de*  
208 *novo* infection, we silenced CTCF in HBV infected HepG2-NTCP cells (Fig.5A). Efficient depletion  
209 of CTCF was demonstrated by western blotting (Fig.5B) and viral RNAs were analysed by RT-

210 qPCR. In agreement with our earlier data with HepG2-HBV-Epi cells, CTCF depletion in this *de*  
211 *novo* infection model increased preC/pgRNA levels and total HBV RNA (**Fig.5C and D**). Moreover,  
212 no significant differences were observed in preS1, preS2 and HBx RNAs (**Fig.5E**). These data  
213 support a model where CTCF represses HBV cccDNA transcription, the major transcriptional  
214 template in *de novo* infected HepG2-NTCP cells. Taken together, our findings provide evidence  
215 that CTCF represses the BCP activity and hence preC/pgRNA levels.

216 **Mutation of CTCF binding sites within HBV Enhancer I increases transcription.** To demonstrate a  
217 direct role for CTCF binding to and regulating cccDNA transcription we utilised the HBV  
218 minicircle (mCHBV) technology, that recapitulates HBV cccDNA transcription and replication  
219 (51). We mutated CTCF BS1 and BS2 alone or in combination in the mCHBV as described in  
220 **Fig.3A**. HepG2-NTCP cells were transfected with wild type mCHBV (WT) or mutant mCHBV;  
221 BS1m, BS2m or BS1/2m, and harvested 3 days post transfection (**Fig.6A**). Analysis of CTCF  
222 binding by ChIP revealed that mutation of BS1 or BS2 alone significantly reduced CTCF binding  
223 by over >75% with the combined mutation resulting in an almost complete loss of CTCF-mCHBV  
224 complexes (**Fig.6B**). qPCR analysis showed a significant increase in preC/pgRNA levels when  
225 either or both of the CTCF BS were mutated (**Fig.6C**). However, no differences were observed  
226 in HBV mcDNA levels, confirming comparable transfection efficiencies (**Fig.6D**). These data  
227 provide strong evidence of direct recruitment of CTCF to HBV DNA and show the repressive  
228 role for CTCF in regulating HBV transcription.

229

## 230 DISCUSSION

231 In this study we identified two CTCF-binding motifs within transcription regulatory elements,  
232 EnhI and Xp, of the HBV genome. We demonstrate CTCF binding to HBV DNA using various  
233 model systems that bear both integrated genomes and a cccDNA pool, or cells exclusively  
234 expressing episomal copies of viral DNA. Our sonication method sheared cccDNA-like episomes  
235 allowing provisional mapping of CTCF binding sites that were confirmed by mutagenesis studies  
236 using promoter reporter constructs and mCHBV DNA. Importantly, these CTCF binding sites are  
237 conserved amongst all HBV genotypes and across the wider *hepadnaviridae* family, consistent  
238 with an evolutionary conserved role in the replication of these viruses. Finally, we show a role  
239 for CTCF to repress HBV transcription.



240 Using several complementary HBV replication models we show that siRNA depletion of CTCF  
241 and mutation of CTCF binding sites significantly increase preC/pgRNA levels, consistent with a  
242 role for CTCF in repressing viral transcription. To understand the mechanism of CTCF action we  
243 used transcriptional reporter assays and found that silencing CTCF significantly increased EnhI  
244 activity. Furthermore, mutating the CTCF BS within EnhI attenuated this phenotype, confirming  
245 a direct role for CTCF in regulating EnhI. However, analysis of the full BCP, containing both EnhI  
246 and EnhII, revealed that the phenotype of CTCF silencing was lost. It is likely that the  
247 attenuation of BCP activity following CTCF silencing is explained by the dominant repressive  
248 effects of the NRE within EnhII, highlighting the context dependent activity of CTCF in regulating  
249 HBV. However, increased activity of the BCP is observed following CTCF silencing in cells  
250 containing the full viral episome, which may reflect differential chromatinization and epigenetic  
251 modification of the transcriptional reporters as compared to the full viral episome.  
252 Alternatively, the transcriptional elements in isolation are no longer subject to regulation by  
253 distal elements contained within the intact episome.

254 To confirm a direct role of CTCF in repressing HBV transcription, we transfected HepG2-NTCP  
255 cells with mcHBV mutated in the CTCF BSs. Although the extent to which we could mutate CTCF  
256 BS was limited, to maintain the amino acid sequence of the polymerase, we observed a  
257 significant reduction of CTCF binding to mcHBV lacking either BS1 or BS2, or both sites mutated  
258 in combination. These studies identify the CTCF BSs within the viral genome and confirm CTCF  
259 association with HBV DNA. Consistent with the increased preC/pgRNA levels observed in two  
260 HBV replication model systems following CTCF depletion, we observed a significant increase in  
261 preC/pgRNA when CTCF BS1 was mutated. A similar increase in preC/pgRNA was observed  
262 when CTCF BS2 was mutated although this did not reach statistical significance. While the  
263 mutation of both BS showed a significant increase in preC/pgRNA abundance, suggesting these  
264 sites do not function in a synergistic manner within this model system.

265 Integration of the HBV genome into the host genome frequently occurs in persistent infection,  
266 presumably due to formation of linear double-stranded HBV DNA during aberrant virus  
267 replication (52). HBV genome integration is not part of the productive HBV life cycle and the  
268 estimated frequency is relatively low (<1 copy per diploid host genome in infected tissues) (53).  
269 However, HBV integration can cause host genomic instability leading to tumour progression  
270 through tumour suppressor gene inactivation and/or oncogene activation (54). Oncogenic

271 integration events are thought to provide a growth advantage to cells, inducing tumourigenesis  
272 (55). HBV integration occurs at random sites, although a preference for integration within  
273 regions of open chromatin has been reported (56). It will be interesting to determine whether  
274 integration of HBV DNA into the host results in an alteration of local chromatin interactions and  
275 host cell gene regulation by the insertion of a virally encoded CTCF binding site(s), as reported  
276 for the human retrovirus, HTLV-1 (57). Such genomic rearrangements could have a dramatic  
277 effect on host cell gene expression and contribute to HBV-driven carcinogenesis.

278 Analysis of the epigenetic status of HBV DNA in HepG2.2.15 hepatoma cells revealed a lack of  
279 the repressive H3K27Me3 and enrichment of epigenetic marks associated with active  
280 transcription in the Xp and BCP regions, downstream of the CTCF binding sites in EnhI/Xp.  
281 Similar enrichment of H4Ac was observed in episomal DNA in HepG2-HBV-Epi cells. These  
282 findings are consistent with previous reports studying the epigenetic status of HBV cccDNA in  
283 various model systems and liver biopsy samples (19, 20). Silencing of CTCF resulted in an  
284 increase in H4Ac abundance in HBV cccDNA, which associates with increased HBV preC/pgRNA  
285 levels.

286 Taken together, these findings suggest that CTCF represses HBV transcription by insulating the  
287 BCP from the upstream enhancer element, EnhI. EnhI is an important regulator of all HBV  
288 promoters and is essential for viral transcription (58, 59). In support of this, HBV-transgenic  
289 mice lacking EnhI are defective in virion production (60). The repression of EnhI by CTCF is likely  
290 to have a significant impact on the virus life cycle and reduce particle genesis and thereby limit  
291 cccDNA pools. Having identified CTCF as a repressor of HBV, we hypothesised that chronic HBV  
292 infection may perturb CTCF expression. However, analysing publically available Affymetrix  
293 microarray database (61) we found no evidence for HBV infection to perturb intra-hepatic CTCF  
294 transcript levels (**Sup Fig.S2**).

295 Analysis of the genomic distribution of CTCF BS in the human genome suggests a similar  
296 enhancer-blocking activity of CTCF as numerous CTCF binding loci are situated between known  
297 transcriptional enhancers and associated promoter elements (62). Such enhancer blocking  
298 activity has been extensively characterised at imprinted loci such as the insulin-like growth  
299 factor 2 (IGF2)/H19 locus and in development at the  $\beta$ -globin locus (63, 64). CTCF regulates  
300 herpes simplex virus differential transcriptional programmes during the lytic and latent phases  
301 of the viral life cycle through its enhancer-blocking activity (38). CTCF has been reported to

302 directly repress transcription via recruitment of the Sin3/histone deacetylase (HDAC)  
303 compressor complex resulting in reduced histone acetylation (65) that may explain our  
304 observations showing increased H4Ac of HBV DNA following CTCF silencing. Our previous work  
305 in HPV demonstrated that CTCF represses transcription by stabilising an epigenetically  
306 repressed chromatin loop between the viral proximal enhancer and a distal CTCF binding site.  
307 However, this repression was not associated with direct binding of CTCF to the HPV enhancer,  
308 suggesting that HBV and HPV have evolved fundamentally different mechanisms of CTCF-  
309 dependent transcriptional repression.

310

## 311 **METHODS**

312 **Cell lines and antibodies.** HepG2.2.15 (41), HepAD38 (42), HepG2-HBV-Epi (43) and HepG2-  
313 NTCP cells (48) were maintained in Dulbecco's Modified Eagles Medium (DMEM, #31966)  
314 supplemented with 10% fetal bovine serum (FBS), 2 mM L-glutamine, 1 mM sodium pyruvate,  
315 50 U.mL<sup>-1</sup> penicillin/streptomycin and non-essential amino acids (all reagents from Invitrogen,  
316 UK). All cells were maintained in a 5% CO<sub>2</sub> atmosphere at 37°C. HepG2-HBV-Epi cells were kept  
317 at low passage to limit HBV DNA integration. The following primary antibodies were used: anti-  
318 CTCF (#61311), anti-H3K4Me3 (#39915), anti-H3K27Me3 (#39155) and anti-H4Ac (#39925)  
319 were all purchased from Active motif (UK) and anti-GAPDH (SC-32233) was purchased from  
320 Santa Cruz.

321 **ChIP and quantitative PCR.** HepG2.215, HepAD38 cells or HepG2-HBV-Epi cells were fixed with  
322 1% formaldehyde (Sigma Aldrich) for 10 min at room temperature before quenching with 125  
323 mM glycine. Cells were washed with ice cold PBS containing EDTA-free protease inhibitors  
324 (Roche) and 5 mM sodium butyrate and frozen at -80°C. Pellets were resuspended in ChIP lysis  
325 buffer (Active Motif) supplemented with protease inhibitors and incubated on ice for 30 mins.  
326 Cells were dounced 30 times using the tight pestle to release nuclei and centrifuged at 2500  
327 xg for 10 mins at 4°C. The supernatant was removed and discarded. Nuclei were resuspended  
328 in shearing buffer (Active Motif) pulse sonicated using a Sonics Vibra Cell CV18 sonicator fitted  
329 with a micro-probe at 25% amplitude for 15 min on ice using 30 sec on/off cycles. Chromatin  
330 samples were cleared by centrifugation and stored at -80°C.

331 Sonication of HBV cccDNA was evaluated by conventional PCR amplification of increasing  
332 amplicon size using a constant sense primer and anti-sense primers described in **Table 1**.  
333 Phenol-chloroform extracted DNA from HepG2-HBV-Epi cells before and after sonication was  
334 quantified using a NanoDrop ND-1000 spectrophotometer. PCR reactions included 100 ng  
335 DNA, MyTaq Red PCR Mix (Bioline, UK) and 200 nM sense/anti-sense primers and amplification  
336 following 35 cycles of 95°C, 15 secs; 55°C, 15 secs; 72°C, 30 secs assessed by agarose gel  
337 electrophoresis. Products were visualised using SyBr Green Safe dye (Invitrogen).

338 For ChIP, sonicated lysates were clarified by centrifugation at 16,000 xg for 10 min and CTCF  
339 or histone complexes immunoprecipitated with 5-8 µg antibody using a ChIP-IT® Express  
340 Chromatin Immunoprecipitation kit, including Protein A magnetic beads as per manufacturer's  
341 instructions (Active Motif, USA). The input and immunoprecipitated DNA were quantified by  
342 real-time PCR using a Stratagene MX3500P PCR System. The values were calculated as %  
343 recovery respective to input DNA signals. All oligonucleotide sequences are listed in **Table 1**.

344 **siRNA transfection.** Cells were trypsinized to reverse transfect with 25nM of CTCF-specific or  
345 scrambled TARGETplus Smartpool siRNAs (Horizon, USA) using DharmaFECT4 (20% of amount  
346 recommended by the manufacturer's protocol; Fisher Scientific, Dharmacon). Cells with no  
347 siRNA (un-treated; UT) were also assayed to assess lethality of CTCF depletion.

348 **SDS-PAGE and western blots.** Cells were lysed in urea lysis buffer (8M urea, 150mM NaCl, 20  
349 mM Tris, pH 7.5, 0.5 M β-mercaptoethanol) supplemented with protease inhibitor cocktail  
350 (Roche) and sonicated for 10 s at 20% amplitude using a Sonics Vibra Cell sonicator fitted with  
351 a microprobe. Following quantification of protein concentration by Bradford assay, samples  
352 were diluted in Lamelli buffer before incubating at 95°C for 5 min. Proteins were separated on  
353 a 10 % polyacrylamide gel and transferred to PVDF membranes (Amersham). The membranes  
354 were blocked in TBS-T, 5 % skimmed milk, and proteins detected using specific primary (diluted  
355 at 1:1000) and HRP-secondary antibodies (ThermoFisher, diluted at 1:10,000). Protein bands  
356 were detected using Pierce SuperSignal West Pico chemiluminescent substrate kit (Pierce) and  
357 images collected using a Fusion FX Imaging system (Peqlab).

358 **HBV transcription reporter assays.**  $1 \times 10^5$  HepG2-NTCP cells were seeded in collagen-coated 24-  
359 well plates. Immediately following cell seeding, transfection mixes were added containing 100  
360 ng of either pGL3b-Enh1, pGL3b-BCP or pGL3b-basic, 25 ng *Renilla* luciferase control plasmid

361 (pCMV-Renilla), 25 nM scrambled or CTCF-specific siRNA and 1.5 µl Lipofectamine RNAiMAX™  
362 (ThermoFisher Scientific) in 100 µl OptiMEM (ThermoFisher Scientific). Cells were incubated  
363 at 37°C, 5 % CO<sub>2</sub> for 72 h before being washed with PBS and 200 µL Passive Lysis buffer  
364 (Promega, UK) added to each well. Samples were incubated at RT for 30 min with gentle  
365 rocking. Lysates were cleared by centrifugation and 20 µL of each added to a white 96-well  
366 microtitre plate. FireFly and *Renilla* Luciferase activity were detected using the Dual-  
367 Luciferase® Reporter Assay (Promega, UK) using a GloMAX®-Multi Detection system (Promega,  
368 UK). 50 µL reagent added at a speed of 200 µl/s followed by mixing and 2 s delay. Integration  
369 time was 10 s with 1 read/well for Firefly luciferase detection. The same protocol was used for  
370 subsequent *Renilla* luciferase detection. Normalised luciferase activity was calculated by  
371 dividing Firefly luciferase activity by *Renilla* luciferase activity.

372 **HBV *de novo* infection.** Purified HBV was produced from HepAD38 cells as previously reported  
373 (48). HepG2-NTCP cells were seeded on collagen-coated plasticware and infected with HBV at  
374 an MOI of 250 genome equivalents per cell in the presence of 4% polyethylene glycol 8,000.  
375 Viral inoculum was removed 8 h post infection by extensive washing with PBS and cells  
376 maintained in DMSO-free DMEM.

377 **RNA isolation for cDNA synthesis.** Total cellular RNA was extracted using an RNeasy mini kit  
378 (Qiagen) following the manufacturer's protocol. To remove any residual HBV DNA, samples  
379 were treated with RNase-Free DNase I (14 Kunitz units/rxn, Qiagen) for 30 min at RT. RNA  
380 concentration and quality were assessed using a NanoDrop 1000 spectrophotometer (Thermo  
381 Scientific) and 2100 Bioanalyzer (Agilent). cDNA synthesis was performed with 0.25-1 µg of  
382 RNA in a 20 µL total reaction volume using a random hexamer/oligo dT strand synthesis kit as  
383 per the manufacturer's instructions (10 min at 25°C; 15 min at 42°C; 15 min at 48°C; SensiFast,  
384 Biorline). All oligonucleotide sequences are listed in **Table 1**.

385 **Quantitative PCR of HBV transcripts.** All PCR reactions were performed using a SYBR green real-  
386 time PCR protocol (qPCRBIO SyGreen, PCR Biosystems) in a Lightcycler 96™ instrument  
387 (Roche). The amplification conditions were: 95°C for 2 min (enzyme activation), followed by 45  
388 cycles of amplification (95°C for 5 s; 60°C for 30 s). A melting curve analysis was performed on  
389 the completed reactions to assess specificity and purity of the amplicons (95°C for 10 s; 60°C  
390 for 60 s; followed by gradual heating from 60°C to 97°C at 1 °C/s). DNase-treated RNA samples

391 that had not been reverse transcribed were amplified to verify the absence of residual DNA  
392 contamination. All oligonucleotide sequences are listed in **Table 1**.

393 **HBV mcDNA purification and transfection into cells.** The plasmid pMC-HBV contains the 1.0 HBV  
394 genome (awy) and has been previously described (51). CTCF BS1 and CTCF BS2 were mutated  
395 by site-directed PCR mutagenesis using the primers detailed in Table 1 and Prime Star Max  
396 (Takara) mutagenesis kit following the manufacturer's protocols and confirmed by sequencing.  
397 ZYCY10P3S2T competent bacteria (System Bioscience) were then transformed with the pMC-  
398 HBV (WT, BS1m, BS2m or BS1/2m) and a single colony amplified in Terrific Broth overnight at  
399 37°C. 2 volumes of LB medium supplemented with 0.04 N NaOH and 0.02 % L-Arabinose were  
400 added to the culture and further incubated for 8 h at 37°C. Plasmid DNA was extracted using  
401 the Nucleobond Xtra Maxi kit according to the manufacturer's protocol (Macherey-Nagel) and  
402 digested with *NdeI* (New England Biolabs) for 2 h at 37°C and plasmid-safe DNase (System  
403 Bioscience) overnight at 37°C. After purification, plasmid DNA was assessed by agarose gel  
404 electrophoresis to check for elimination of the parental plasmid. HepG2-NTCP cells at 80-90 %  
405 confluency were transfected with the pMC-HBV plasmids using TransIT-2020 (Mirus) according  
406 to the manufacturer's protocol in DMEM supplemented with 5 % FBS, 1 % Glutamax and 1 %  
407 sodium pyruvate. The following day, cells were washed once with PBS and cultured for 72 h in  
408 DMEM supplemented with 5 % FBS, 1 % Glutamax, 1 % sodium pyruvate and 1 %  
409 penicillin/streptomycin.

410 **HBV nucleic acid quantification from mcHBV-transfected cells.** Total DNA was extracted using  
411 MasterPure™ Complete DNA Purification Kit (Epicentre). Total RNA was extracted using  
412 ExtractAll TRI-Reagent (Sigma Aldrich), precipitated in isopropanol, washed in ethanol and  
413 resuspended in RNase-free water. Extracted RNA was digested with RNase-free DNase I  
414 (Qiagen) and cDNA synthesised using SuperScript III reverse transcriptase (Invitrogen,  
415 Carlsbad, USA). cccDNA was quantified after *ExoI* + *ExoIII* endonuclease (Epicentre) digestion  
416 of total extracted DNA for 2 hours at 37°C, followed by 20 minutes inactivation at 80°C. Real-  
417 time qPCR for total HBV DNA and cccDNA was performed using an Applied QuantStudio 7  
418 machine (BioSystem) and TaqMan Advanced Fast Master Mix. Total HBV DNA was quantified  
419 using the TaqMan assay Pa03453406\_s1; cccDNA specific primers and probes were: forward  
420 5'- CCGTGTGCACTTCGCTTCA-3'; reverse 5'- GCACAGCTTGGAGGCTTGA-3' TaqMan probe  
421 [6FAM]CATGGAGACCACCGTGAACGCCC[BBQ] (66). Serial dilutions of a plasmid containing an

422 HBV monomer (pHBV-*EcoRI*) served as quantification standard for total HBV DNA and cccDNA.  
423 The number of cellular genomes was determined by using the  $\beta$ -globin TaqMan assay  
424 Hs00758889\_s1 (Thermo Fisher Scientific, Waltham, MA, USA). preC/pgRNA was quantified  
425 using the following primers and probe: forward 5'- GGAGTGTGGATTGCGACTCCT-3'; reverse 5'-  
426 AGATTGAGATCTTCTGCGAC-3' and TaqMan probe  
427 [6FAM]AGGCAGGTCCTTAGAAGAAGAACTCC[BBQ] (66). Relative amount was normalized over  
428 the expression of housekeeping gene GUSB (Hs99999908\_m1, Thermo Fisher Scientific,  
429 Waltham, MA, USA).

430 **Chromatin immunoprecipitation from mcHBV-transfected cells.** 72h after mcHBV transfection,  
431 cells were washed twice with PBS and cross-linked with 1 % formaldehyde for 10 minutes at  
432 37°C. After 5 minutes quenching with 125 mM glycine at 37°C, cells were washed twice with  
433 PBS, centrifuged for 5 mins at 300 xg and incubated with Nuclear Lysis Buffer (5 mM PIPES, 85  
434 mM KCl, 0.5% NP-40) for 30 minutes on ice to isolate nuclei. The lysate was then dounced 10  
435 times and centrifuged for 5 minutes at 800 xg at 4°C. Nuclear membranes were then broken  
436 by 2 cycles of sonication 30 sec ON, 30 sec OFF on a Bioruptor (Diagenode). Debris were  
437 pelleted 10 mins at 11000 xg at 4°C. The supernatant was diluted 10 times with RIPA buffer (10  
438 mM Tris-HCl pH 7.5, 140 mM NaCl, 1 mM EDTA, 0.5 mM EGTA, 1 % Triton X-100, 0.1 % SDS,  
439 0.1 % Na-deoxycholate) supplemented with Complete Mini EDTA-free protease inhibitor  
440 (Roche Diagnostics) and 1 mM PMSF and pre-cleared for 2h at 4°C by adding magnetic Protein  
441 G Dynabeads (Life Technologies). Beads were discarded and 1  $\mu$ g of anti-CTCF antibody  
442 (Diagenode #C15410210) or isotype matched negative control were added to the chromatin.  
443 After an overnight incubation at 4°C, magnetic Protein G Dynabeads and samples incubated  
444 for 2 h at 4°C with agitation. Beads were washed 5 times with RIPA buffer, once with TE buffer  
445 and resuspended in Elution buffer (20 mM Tris-HCl pH 7.5, 5 mM EDTA, 50 mM NaCl, 1 % SDS,  
446 50  $\mu$ g/ml proteinase K). Chromatin was reverse crosslinked by incubation at 68°C for 2 h and  
447 purified by phenol:chloroform:isoamyl alcohol 25:24:1 (Life Technologies) extraction and  
448 ethanol precipitation. cccDNA was quantified using the primers and probes listed above (66).

449

450 **Acknowledgements:** We acknowledge Stephan Urban (University of Heidelberg, Germany) for  
451 providing HepG2-NTCP cells; Ulrika Protzer (TUM, Germany) for providing HepG2-HBV-Epi cells  
452 and Wang-Shick Ryu (Yonsei University, South Korea) for HBV promoter-transcription reporter

453 plasmids. We thank Claudia Orbegozo Rubio for expert technical assistance and Chunkyu Ko  
454 for advice on HBV biology. BT laboratory is funded by the French Agence nationale de  
455 recherche sur le sida et les hépatites virale (ANRS) ECTZ75178. JAM laboratory is funded by  
456 Wellcome Trust IA 200838/Z/16/Z and MRC project grant MR/R022011/1. JLP laboratory is  
457 funded by MRC project grants MR/R022011/1, MR/T015985/1 and MR/N023498/1. The  
458 funders had no role in study design, data collection and interpretation, or the decision to  
459 submit the work for publication.

460

461 **Author contributions:** VDP conducted experiments; JF conducted experiments; GG conducted  
462 experiments, FC conducted experiments; PACW conducted experiments; JMH conducted  
463 experiments; AC conducted experiments; SB conducted experiments; XZ conducted  
464 experiments; PB performed genetic analysis; BT designed experiments and edited manuscript;  
465 JAM designed experiments and co-wrote manuscript; JLP designed experiments and co-wrote  
466 the manuscript.

467 **Conflict of interest.** None of the authors have any conflict of interest.

468

## 469 FIGURE LEGENDS

470 **Figure 1: CTCF associates with HBV DNA and is enriched at viral Enhancer I and X promoter.** (A)  
471 Association of CTCF with HBV DNA in HepG2.2.15 and HepAD38 cells was analysed by ChIP-  
472 qPCR and presented as % Input recovery. Statistical significance shows comparison of CTCF-  
473 specific ChIP with maximal recovery using IgG control (dotted line). (B) The distribution of  
474 histone modifications (H3K4Me3, H3K27Me3 and H4Ac) in HepG2.2.15 cells by ChIP-qPCR. (C)  
475 Efficiency of chromatin shearing in HepG2-HBV-Epi cells was assessed by PCR of sonicated  
476 versus non-sonicated chromatin. Amplicons were generated with a constant sense primer  
477 (anneals at nt 69) and anti-sense primers binding at increasing distance from the sense primer  
478 (nt 159, 307, 422, 653 and 801). Amplification of HBV DNA was assessed by SyBr green staining  
479 of bands separated by electrophoresis. (D) Association of CTCF was assessed by ChIP-qPCR. (A,  
480 B and D) Data shown are the mean +/- SEM of three technical repeats and are representative  
481 of three biological repetitions. P values were determined using a paired t test. \*denotes p



482 <0.05, \*\*denotes  $p < 0.01$ , \*\*\*denotes  $p < 0.001$ . Annotation of HBV genome features including  
483 open reading frames, enhancers and selected promoters is shown below the histograms.

484 **Figure 2: Identification of conserved CTCF binding sites in HBV genomes and diverse**  
485 ***hepadnaviridae*.** (A) Conservation of CTCF BS among 7,313 HBV sequences (HBVdb.fr). All sites,  
486 except where indicated, are > 98% conserved. (B) Neighbor-joining phylogenetic tree of  
487 members of the *hepadnaviridae* (adapted from (1)). The green box shows viral genomes that  
488 encode both CTCF BS1 and 2 (all human and old world primate viruses), whereas the blue box  
489 shows viral genomes encoding only CTCF BS1 (new world monkeys, woodchucks and all bats  
490 except the tent making bat).

491 **Figure 3: CTCF represses HBV Enhancer I activity.** (A) Depiction of HBV genome regions cloned  
492 upstream of Firefly luciferase in transcriptional reporter plasmids and mutagenesis strategy of  
493 CTCF BS1 and BS2 showing viral enhancers, Xp and BCP, and CTCF BS 1 (blue) and CTCF BS 2  
494 (green). (B) Activity of pEnhi-Luc and pBCP-Luc reporters in HepG2-NTCP cells normalized to  
495 co-transfected *Renilla* luciferase expression plasmid. (C) Western blot showing depletion of  
496 CTCF following siRNA transfection in pEnhi-Luc and pBCP-Luc transfected HepG2-NTCP cells.  
497 (D) Firefly luciferase activity normalized to *Renilla* Luciferase expression in HepG2-NTCP cells  
498 co-transfected with pGL3-basic, pEnhi-Luc or pBCP-Luc and either scrambled (Scr) or CTCF-  
499 specific siRNA duplexes. (E) Normalized luciferase activity in HepG2-NTCP cells transfected  
500 pEnhi-Luc containing mutations in CTCF binding site 1 (BS1m) or 2 (BS2m) or a combination of  
501 both (BS1/2m). Data shown are the mean +/- SEM of three independent repetitions. P values  
502 were determined by the Sidak's ANOVA multiple comparisons test. \*\*\*denotes  $p < 0.001$ .

503 **Figure 4: CTCF represses preC/pgRNA transcription from HBV cccDNA.** HepG2-HBV-Epi cells  
504 were untransfected (UT) or transfected with scrambled (Scr) or CTCF-specific siRNA duplexes  
505 and incubated for 72 h. (A) CTCF depletion was assessed by western blotting and quantification  
506 in three independent experiments shown (B). (C, D) preC/pgRNA and total HBV RNA abundance  
507 were analysed by 4T-qPCR as previously described (46). Data are the mean +/- SD of two  
508 independent experiments performed in triplicate. Data are the mean +/- SEM of two  
509 independent experiments performed in triplicate. P values were determined by the Kruskal-  
510 Wallis ANOVA multiple group comparison. (E) Enrichment of H4Ac marks was assessed by ChIP-  
511 qPCR and shown as % Input recovery. P values were determined using a paired t test. \*denotes  
512  $p < 0.05$ , \*\*denotes  $p < 0.01$ , \*\*\*denotes  $p < 0.001$ .

513 **Figure 5: CTCF represses HBV preC/pgRNA transcription in *de novo* infected HepG2-NTCP cells.**

514 (A) HBV infected HepG2-NTCP were transfected with scrambled (Scr) or CTCF-specific siRNA  
515 duplexes and cultured for 72 h. (B) CTCF depletion was assessed by western blotting and (C)  
516 viral transcript abundance analysed by q4T-PCR as previously described (46). Data are the  
517 mean +/- SD of two independent experiments performed in triplicate. P values were  
518 determined using the Mann-Whitney test (two group comparisons). \*denotes  $p < 0.05$ ,  
519 \*\*denotes  $p < 0.01$ .

520 **Figure 6: Mutation of CTCF binding sites in HBV mcDNA results in increased preC/pgRNA levels.**

521 (A) HepG2-NTCP cells were transfected with wild type HBV mcDNA (WT) or mcDNA with CTCF  
522 binding 1 (BS1m) or 2 (BS2m) or both sites mutated in combination (BS1/2m). (B) Cells were  
523 harvested 72 h post transfection and CTCF binding analysed by ChIP-qPCR and presented as %  
524 of enrichment relative to input chromatin. preC/pgRNA (C) and total HBV DNA (D) levels were  
525 quantified by qRT-PCR and normalized to cccDNA amount per cell to account for mCHBV  
526 transfection efficiency. Data are the mean +/- SEM of at least three independent experiments.  
527 P values were determined using the Kruskal–Wallis ANOVA multiple group comparison.  
528 \*denotes  $p < 0.05$ , \*\*denotes  $p < 0.01$ .

529 **Supplementary figure 1. CTCF levels are reduced in DMSO treated HepG2 cells.**

530 (A) HepG2-NTCP cells were cultured with (+) or without (-) 2.5 %DMSO for 72 h. CTCF protein levels were  
531 assessed by western blotting alongside GAPDH loading control. (B) The relative expression of  
532 CTCF compared to GAPDH was quantified by densitometry. Data are the mean +/- SD of three  
533 independent experiments.

534 **Supplementary figure 2: CTCF expression levels in chronic hepatitis B.**

535 (A) CTCF RNA levels were determined by high density Affymetrix microarray from liver biopsy samples in non-cirrhotic  
536 HBV infected patients (61). Patients with detectable peripheral HBV DNA (n=90) were  
537 compared against healthy patient samples (n=6). Statistical analysis was carried out using  
538 Mann-Whitney U test. (B) HBV infected patients were categorised into 2 groups based on low  
539 (n=36) or high (n=54) peripheral HBV DNA levels, and CTCF expression was compared between  
540 the two groups. Statistical analysis was carried out using the Mann-Whitney U test.

541

542

543 Table 1: Detailing all primer sequences used.

PRIMER PAIR	FORWARD (5' – 3')	REVERSE (5' – 3')
T1	GGGGAACATAATGACTCTAGCTACC	TTTAGGCCCATATTAGTGTTGACA
T2	CAAGGTAGGAGCTGGAGCATTTC	GAGGCAGGAGGCGGATTTG
T3	CTCCAGTTCAGGAACAGTAAACCC	AGGAATCCTGATGTGATGTTCTCC
T4	ACGGGGCGCACCTCTCTTTA	GTGAAGCGAAGTGCACACGG
<b>β-ACTIN</b>	CCAACCGCGAGAAGATGA	CCAGAGGCGTACAGGGATAG
<b>MUTAGENESIS PRIMERS (LUC)</b>		
CTCF BS1	CTGGATGGGGCTTGGTCATGCGC	TTGGTGTTCGCTCAGCAAACACTTGG
CTCF BS2	AGCAGCTTGTTTTGCTCGCAGC	AATAATTCCGCAGTATGGATCGG
<b>MUTAGENESIS PRIMERS (pMC-HBV)</b>		
CTCF BS1	GTGTTTGCTGACGCAACACCAACT- GGATGGGGCTTGGTC	GACCAAGCCCCATCCAGTTGGTGTTCGCT- CAGCAAACAC
CTCF BS2	GCCGATCCATACTGCGGAATTATT- AGCAGCTTGTTTTGCTCGCAGCAGG	CCTGCTGCGAGCAAAAACAAGCTGCTAATA- ATTCCGCAGTATGGATCGGC
<b>HBV CHIP PRIMERS</b>		
178 - 307	TTCCTAGGACCCCTTCTCGT	GGCCAAGACACACGGTAGTT
254 - 428	TCGTGGTGGACTTCTCTCAA	TGAGGCATAGCAGCAGGAT
346 - 422	TCCTGTCTCCAACCTTGTC	AGCAGCAGGATGAAGAGGAA
462 - 562	GTTGCCCGTTTGTCTCTAATTC	GGAGGGATACATAGAGGTTCCCTTGA
518 - 653	GCCGAACCTGCATGACTACT	GCCGAACCTGCATGACTACT
718 - 801	CCCCTGTTTGGCTTTTCAGT	CAGCGGTAAAAAGGGACTCA
995 - 1108	ACGAATTGTGGGTCTTTTGG	GTTGGCGAGAAAAGTAAAAGC
1089 - 1154	GCTTTCACTTTCTCGCCAAC	AACGGGGTAAAGGTTTCAGGT
1305 - 1438	AGCAGGTCTGGAGCAAACAT	GACGGGACGTAAACAAAGGA
1581 - 1693	GTGCACTTCGCTTCACCTCT	GGTCGTTGACATTGCAGAGA
1738 - 1837	GGAGTTGGGGGAGGAGATTA	GGCAGAGGTGAAAAAGTTGC
1901 - 2054	GCATGGACATCGACCCTTAT	TGAGGTGAACAATGCTCAGG
2112 - 2297	CTGGGTGGGTGTTAATTTGG	TAAGCTGGAGGAGTGCGAAT
2279 - 2392	TTCGCACTCCTCCAGCTTAT	GAGGCGAGGGAGTTCTTCTT
2983 - 3133	ACAAGGTAGGAGCTGGAGCA	GTAGGCTGCCTTCTGTCTG
<b>HBV cccDNA SHEARING</b>		
F69 - R159	CTCCAGTTCAGGAACAGTAAACCC	AGGAATCCTGATGTGATGTTCTCC
R307		GGCCAAGACACACGGTAGTT
R422		AGCAGCAGGATGAAGAGGAA
R653		GCCGAACCTGCATGACTACT
R801		CAGCGGTAAAAAGGGACTCA

544

545

546

547

548

549 REFERENCES

- 550 1. McNaughton AL, D'Arienzo V, Ansari MA, Lumley SF, Littlejohn M, Revill P, McKeating  
551 JA, Matthews PC. 2019. Insights From Deep Sequencing of the HBV Genome-Unique,  
552 Tiny, and Misunderstood. *Gastroenterology* 156:384-399.
- 553 2. Sozzi V, Walsh R, Littlejohn M, Colledge D, Jackson K, Warner N, Yuen L, Locarnini SA,  
554 Revill PA. 2016. In Vitro Studies Show that Sequence Variability Contributes to Marked  
555 Variation in Hepatitis B Virus Replication, Protein Expression, and Function Observed  
556 across Genotypes. *J Virol* 90:10054-10064.
- 557 3. Buti M, Elefsiniotis I, Jardi R, Vargas V, Rodriguez-Frias F, Schapper M, Bonovas S,  
558 Esteban R. 2007. Viral genotype and baseline load predict the response to adefovir  
559 treatment in lamivudine-resistant chronic hepatitis B patients. *J Hepatol* 47:366-72.
- 560 4. Kao JH, Chen PJ, Lai MY, Chen DS. 2000. Hepatitis B genotypes correlate with clinical  
561 outcomes in patients with chronic hepatitis B. *Gastroenterology* 118:554-9.
- 562 5. Yan H, Zhong G, Xu G, He W, Jing Z, Gao Z, Huang Y, Qi Y, Peng B, Wang H, Fu L, Song  
563 M, Chen P, Gao W, Ren B, Sun Y, Cai T, Feng X, Sui J, Li W. 2012. Sodium taurocholate  
564 cotransporting polypeptide is a functional receptor for human hepatitis B and D virus.  
565 *Elife* 3.
- 566 6. Ni Y, Lempp FA, Mehrle S, Nkongolo S, Kaufman C, Falth M, Stindt J, Koniger C, Nassal  
567 M, Kubitz R, Sultmann H, Urban S. 2014. Hepatitis B and D viruses exploit sodium  
568 taurocholate co-transporting polypeptide for species-specific entry into hepatocytes.  
569 *Gastroenterology* 146:1070-83.
- 570 7. Hong X, Kim ES, Guo H. 2017. Epigenetic regulation of hepatitis B virus covalently  
571 closed circular DNA: Implications for epigenetic therapy against chronic hepatitis B.  
572 *Hepatology* 66:2066-2077.
- 573 8. Lythgoe KA LS, McKeating JA, Matthews PC. 2020. Estimation of hepatitis B virus  
574 cccDNA persistence in chronic infection using within-host evolutionary rates. medRxiv  
575 02.04.20020362.
- 576 9. Levrero M, Pollicino T, Petersen J, Belloni L, Raimondo G, Dandri M. 2009. Control of  
577 cccDNA function in hepatitis B virus infection. *J Hepatol* 51:581-92.
- 578 10. Stadelmayer B, Diederichs A, Chapus F, Rivoire M, Neveu G, Alam A, Fraisse L, Carter  
579 K, Testoni B, Zoulim F. 2020. Full-length 5'RACE identifies all major HBV transcripts in

- 580 HBV-infected hepatocytes and patient serum. J Hepatol  
581 doi:10.1016/j.jhep.2020.01.028.
- 582 11. Altinel K, Hashimoto K, Wei Y, Neuveut C, Gupta I, Suzuki AM, Dos Santos A, Moreau  
583 P, Xia T, Kojima S, Kato S, Takikawa Y, Hidaka I, Shimizu M, Matsuura T, Tsubota A,  
584 Ikeda H, Nagoshi S, Suzuki H, Michel ML, Samuel D, Buendia MA, Faivre J, Carninci P.  
585 2016. Single-Nucleotide Resolution Mapping of Hepatitis B Virus Promoters in Infected  
586 Human Livers and Hepatocellular Carcinoma. J Virol 90:10811-10822.
- 587 12. Fukai K, Takada S, Yokosuka O, Saisho H, Omata M, Koike K. 1997. Characterization of  
588 a specific region in the hepatitis B virus enhancer I for the efficient expression of X  
589 gene in the hepatic cell. Virology 236:279-87.
- 590 13. Quarleri J. 2014. Core promoter: a critical region where the hepatitis B virus makes  
591 decisions. World J Gastroenterol 20:425-35.
- 592 14. Yuh CH, Ting LP. 1990. The genome of hepatitis B virus contains a second enhancer:  
593 cooperation of two elements within this enhancer is required for its function. J Virol  
594 64:4281-7.
- 595 15. Sun CT, Lo WY, Wang IH, Lo YH, Shiou SR, Lai CK, Ting LP. 2001. Transcription  
596 repression of human hepatitis B virus genes by negative regulatory element-binding  
597 protein/SON. J Biol Chem 276:24059-67.
- 598 16. Li MS, Lau TC, Chan SK, Wong CH, Ng PK, Sung JJ, Chan HL, Tsui SK. 2011. The G1613A  
599 mutation in the HBV genome affects HBeAg expression and viral replication through  
600 altered core promoter activity. PLoS One 6:e21856.
- 601 17. Bock CT, Schranz P, Schroder CH, Zentgraf H. 1994. Hepatitis B virus genome is  
602 organized into nucleosomes in the nucleus of the infected cell. Virus Genes 8:215-29.
- 603 18. Bock CT, Schwinn S, Locarnini S, Fyfe J, Manns MP, Trautwein C, Zentgraf H. 2001.  
604 Structural organization of the hepatitis B virus minichromosome. J Mol Biol 307:183-  
605 96.
- 606 19. Tropberger P, Mercier A, Robinson M, Zhong W, Ganem DE, Holdorf M. 2015. Mapping  
607 of histone modifications in episomal HBV cccDNA uncovers an unusual chromatin  
608 organization amenable to epigenetic manipulation. Proc Natl Acad Sci U S A  
609 112:E5715-24.

- 610 20. Flecken T, Meier MA, Skewes-Cox P, Barkan DT, Heim MH, Wieland SF, Holdorf MM.  
611 2019. Mapping the Heterogeneity of Histone Modifications on Hepatitis B Virus DNA  
612 Using Liver Needle Biopsies Obtained from Chronically Infected Patients. *J Virol* 93.
- 613 21. Dandri M. 2020. Epigenetic modulation in chronic hepatitis B virus infection. *Semin*  
614 *Immunopathol* 42:173-185.
- 615 22. Guerrieri F, Belloni L, D'Andrea D, Pediconi N, Le Pera L, Testoni B, Scisciani C, Floriot  
616 O, Zoulim F, Tramontano A, Levrero M. 2017. Genome-wide identification of direct  
617 HBx genomic targets. *BMC Genomics* 18:184.
- 618 23. Tang H, Oishi N, Kaneko S, Murakami S. 2006. Molecular functions and biological roles  
619 of hepatitis B virus x protein. *Cancer Sci* 97:977-83.
- 620 24. Belloni L, Pollicino T, De Nicola F, Guerrieri F, Raffa G, Fanciulli M, Raimondo G, Levrero  
621 M. 2009. Nuclear HBx binds the HBV minichromosome and modifies the epigenetic  
622 regulation of cccDNA function. *Proc Natl Acad Sci U S A* 106:19975-9.
- 623 25. Chong CK, Cheng CYS, Tsoi SYJ, Huang FY, Liu F, Fung J, Seto WK, Lai KK, Lai CL, Yuen  
624 MF, Wong DK. 2020. HBV X protein mutations affect HBV transcription and association  
625 of histone-modifying enzymes with covalently closed circular DNA. *Sci Rep* 10:802.
- 626 26. Turton KL, Meier-Stephenson V, Badmalia MD, Coffin CS, Patel TR. 2020. Host  
627 Transcription Factors in Hepatitis B Virus RNA Synthesis. *Viruses* 12.
- 628 27. Rowley MJ, Corces VG. 2018. Organizational principles of 3D genome architecture. *Nat*  
629 *Rev Genet* 19:789-800.
- 630 28. Chen H, Tian Y, Shu W, Bo X, Wang S. 2012. Comprehensive identification and  
631 annotation of cell type-specific and ubiquitous CTCF-binding sites in the human  
632 genome. *PLoS One* 7:e41374.
- 633 29. Kumar S, Bucher P. 2016. Predicting transcription factor site occupancy using DNA  
634 sequence intrinsic and cell-type specific chromatin features. *BMC Bioinformatics* 17  
635 *Suppl* 1:4.
- 636 30. Filippova GN, Fagerlie S, Klenova EM, Myers C, Dehner Y, Goodwin G, Neiman PE,  
637 Collins SJ, Lobanenkov VV. 1996. An exceptionally conserved transcriptional repressor,  
638 CTCF, employs different combinations of zinc fingers to bind diverged promoter  
639 sequences of avian and mammalian c-myc oncogenes. *Mol Cell Biol* 16:2802-13.
- 640 31. Pena-Hernandez R, Marques M, Hilmi K, Zhao T, Saad A, Alaoui-Jamali MA, del Rincon  
641 SV, Ashworth T, Roy AL, Emerson BM, Witcher M. 2015. Genome-wide targeting of the

- 642 epigenetic regulatory protein CTCF to gene promoters by the transcription factor TFII-  
643 I. Proc Natl Acad Sci U S A 112:E677-86.
- 644 32. Pentland I, Parish JL. 2015. Targeting CTCF to Control Virus Gene Expression: A  
645 Common Theme amongst Diverse DNA Viruses. *Viruses* 7:3574-85.
- 646 33. Chen HS, Martin KA, Lu F, Lupey LN, Mueller JM, Lieberman PM, Tempera I. 2014.  
647 Epigenetic deregulation of the LMP1/LMP2 locus of Epstein-Barr virus by mutation of  
648 a single CTCF-cohesin binding site. *J Virol* 88:1703-13.
- 649 34. Kang H, Wiedmer A, Yuan Y, Robertson E, Lieberman PM. 2011. Coordination of KSHV  
650 latent and lytic gene control by CTCF-cohesin mediated chromosome conformation.  
651 *PLoS Pathog* 7:e1002140.
- 652 35. Lang F, Li X, Vladimirova O, Hu B, Chen G, Xiao Y, Singh V, Lu D, Li L, Han H,  
653 Wickramasinghe JM, Smith ST, Zheng C, Li Q, Lieberman PM, Fraser NW, Zhou J. 2017.  
654 CTCF interacts with the lytic HSV-1 genome to promote viral transcription. *Sci Rep*  
655 7:39861.
- 656 36. Li DJ, Verma D, Mosbrugger T, Swaminathan S. 2014. CTCF and Rad21 act as host cell  
657 restriction factors for Kaposi's sarcoma-associated herpesvirus (KSHV) lytic replication  
658 by modulating viral gene transcription. *PLoS Pathog* 10:e1003880.
- 659 37. Tempera I, Wiedmer A, Dheekollu J, Lieberman PM. 2010. CTCF prevents the  
660 epigenetic drift of EBV latency promoter Qp. *PLoS Pathog* 6:e1001048.
- 661 38. Washington SD, Musarrat F, Ertel MK, Backes GL, Neumann DM. 2018. CTCF Binding  
662 Sites in the Herpes Simplex Virus 1 Genome Display Site-Specific CTCF Occupation,  
663 Protein Recruitment, and Insulator Function. *J Virol* 92.
- 664 39. Pentland I, Campos-Leon K, Cotic M, Davies KJ, Wood CD, Groves IJ, Burley M, Coleman  
665 N, Stockton JD, Noyvert B, Beggs AD, West MJ, Roberts S, Parish JL. 2018. Disruption  
666 of CTCF-YY1-dependent looping of the human papillomavirus genome activates  
667 differentiation-induced viral oncogene transcription. *PLoS Biol* 16:e2005752.
- 668 40. Paris C, Pentland I, Groves I, Roberts DC, Powis SJ, Coleman N, Roberts S, Parish JL.  
669 2015. CCCTC-binding factor recruitment to the early region of the human  
670 papillomavirus 18 genome regulates viral oncogene expression. *J Virol* 89:4770-85.
- 671 41. Sells MA, Chen ML, Acs G. 1987. Production of hepatitis B virus particles in Hep G2  
672 cells transfected with cloned hepatitis B virus DNA. *Proc Natl Acad Sci U S A* 84:1005-  
673 9.

- 674 42. Ladner SK, Otto MJ, Barker CS, Zaifert K, Wang GH, Guo JT, Seeger C, King RW. 1997.  
675 Inducible expression of human hepatitis B virus (HBV) in stably transfected  
676 hepatoblastoma cells: A novel system for screening potential inhibitors of HBV  
677 replication. *Antimicrobial Agents and Chemotherapy* 41:1715-1720.
- 678 43. Lucifora J, Xia Y, Reisinger F, Zhang K, Stadler D, Cheng X, Sprinzl MF, Koppensteiner  
679 H, Makowska Z, Volz T, Remouchamps C, Chou WM, Thasler WE, Huser N, Durantel D,  
680 Liang TJ, Munk C, Heim MH, Browning JL, Dejardin E, Dandri M, Schindler M,  
681 Heikenwalder M, Protzer U. 2014. Specific and nonhepatotoxic degradation of nuclear  
682 hepatitis B virus cccDNA. *Science* 343:1221-8.
- 683 44. Ko C, Lee S, Windisch MP, Ryu WS. 2014. DDX3 DEAD-box RNA helicase is a host factor  
684 that restricts hepatitis B virus replication at the transcriptional level. *J Virol* 88:13689-  
685 98.
- 686 45. Schmidt D, Schwalie PC, Wilson MD, Ballester B, Goncalves A, Kutter C, Brown GD,  
687 Marshall A, Flicek P, Odom DT. 2012. Waves of retrotransposon expansion remodel  
688 genome organization and CTCF binding in multiple mammalian lineages. *Cell* 148:335-  
689 48.
- 690 46. D'Arienzo V, Magri A, Harris JM, Wing PAC, Ko C, Rubio CO, Revill PA, Protzer U, Balfe  
691 P, McKeating JA. 2019. A PCR assay to quantify patterns of HBV transcription. *J Gen  
692 Virol* doi:10.1099/jgv.0.001373.
- 693 47. Pollicino T, Belloni L, Raffa G, Pediconi N, Squadrito G, Raimondo G, Levrero M. 2006.  
694 Hepatitis B virus replication is regulated by the acetylation status of hepatitis B virus  
695 cccDNA-bound H3 and H4 histones. *Gastroenterology* 130:823-37.
- 696 48. Ko C, Chakraborty A, Chou WM, Hasreiter J, Wettengel JM, Stadler D, Bester R, Asen  
697 T, Zhang K, Wisskirchen K, McKeating JA, Ryu WS, Protzer U. 2018. Hepatitis B virus  
698 genome recycling and de novo secondary infection events maintain stable cccDNA  
699 levels. *J Hepatol* 69:1231-1241.
- 700 49. Villa P, Arioli P, Guitani A. 1991. Mechanism of maintenance of liver-specific functions  
701 by DMSO in cultured rat hepatocytes. *Exp Cell Res* 194:157-60.
- 702 50. Zvibel I, Fiorino AS, Brill S, Reid LM. 1998. Phenotypic characterization of rat hepatoma  
703 cell lines and lineage-specific regulation of gene expression by differentiation agents.  
704 *Differentiation* 63:215-23.



- 705 51. Yan ZP, Zeng J, Yu YJ, Xiang KL, Hu H, Zhou X, Gu LL, Wang L, Zhao J, Young JAT, Gao L.  
706 2017. HBVcircle: A novel tool to investigate hepatitis B virus covalently closed circular  
707 DNA. *Journal of Hepatology* 66:1149-1157.
- 708 52. Habig JW, Loeb DD. 2003. Template switches during plus-strand DNA synthesis of duck  
709 hepatitis B virus are influenced by the base composition of the minus-strand terminal  
710 redundancy. *J Virol* 77:12412-20.
- 711 53. Podlaha O, Wu G, Downie B, Ramamurthy R, Gaggar A, Subramanian M, Ye Z, Jiang Z.  
712 2019. Genomic modeling of hepatitis B virus integration frequency in the human  
713 genome. *PLoS One* 14:e0220376.
- 714 54. Zhao LH, Liu X, Yan HX, Li WY, Zeng X, Yang Y, Zhao J, Liu SP, Zhuang XH, Lin C, Qin CJ,  
715 Zhao Y, Pan ZY, Huang G, Liu H, Zhang J, Wang RY, Yang Y, Wen W, Lv GS, Zhang HL,  
716 Wu H, Huang S, Wang MD, Tang L, Cao HZ, Wang L, Lee TL, Jiang H, Tan YX, Yuan SX,  
717 Hou GJ, Tao QF, Xu QG, Zhang XQ, Wu MC, Xu X, Wang J, Yang HM, Zhou WP, Wang  
718 HY. 2016. Genomic and oncogenic preference of HBV integration in hepatocellular  
719 carcinoma. *Nat Commun* 7:12992.
- 720 55. Ding D, Lou X, Hua D, Yu W, Li L, Wang J, Gao F, Zhao N, Ren G, Li L, Lin B. 2012.  
721 Recurrent targeted genes of hepatitis B virus in the liver cancer genomes identified by  
722 a next-generation sequencing-based approach. *PLoS Genet* 8:e1003065.
- 723 56. Furuta M, Tanaka H, Shiraishi Y, Unida T, Imamura M, Fujimoto A, Fujita M, Sasaki-Oku  
724 A, Maejima K, Nakano K, Kawakami Y, Arihiro K, Aikata H, Ueno M, Hayami S, Ariizumi  
725 SI, Yamamoto M, Gotoh K, Ohdan H, Yamaue H, Miyano S, Chayama K, Nakagawa H.  
726 2018. Characterization of HBV integration patterns and timing in liver cancer and HBV-  
727 infected livers. *Oncotarget* 9:25075-25088.
- 728 57. Melamed A, Yaguchi H, Miura M, Witkover A, Fitzgerald TW, Birney E, Bangham CR.  
729 2018. The human leukemia virus HTLV-1 alters the structure and transcription of host  
730 chromatin in cis. *Elife* 7.
- 731 58. Antonucci TK, Rutter WJ. 1989. Hepatitis B virus (HBV) promoters are regulated by the  
732 HBV enhancer in a tissue-specific manner. *J Virol* 63:579-83.
- 733 59. Hu KQ, Siddiqui A. 1991. Regulation of the hepatitis B virus gene expression by the  
734 enhancer element I. *Virology* 181:721-6.
- 735 60. Guidotti LG, Matzke B, Schaller H, Chisari FV. 1995. High-level hepatitis B virus  
736 replication in transgenic mice. *J Virol* 69:6158-69.

- 737 61. Zhou W, Ma Y, Zhang J, Hu J, Zhang M, Wang Y, Li Y, Wu L, Pan Y, Zhang Y, Zhang X,  
738 Zhang X, Zhang Z, Zhang J, Li H, Lu L, Jin L, Wang J, Yuan Z, Liu J. 2017. Predictive model  
739 for inflammation grades of chronic hepatitis B: Large-scale analysis of clinical  
740 parameters and gene expressions. *Liver Int* 37:1632-1641.
- 741 62. Xie X, Mikkelsen TS, Gnirke A, Lindblad-Toh K, Kellis M, Lander ES. 2007. Systematic  
742 discovery of regulatory motifs in conserved regions of the human genome, including  
743 thousands of CTCF insulator sites. *Proc Natl Acad Sci U S A* 104:7145-50.
- 744 63. Bell AC, West AG, Felsenfeld G. 1999. The protein CTCF is required for the enhancer  
745 blocking activity of vertebrate insulators. *Cell* 98:387-96.
- 746 64. Chung JH, Whiteley M, Felsenfeld G. 1993. A 5' element of the chicken beta-globin  
747 domain serves as an insulator in human erythroid cells and protects against position  
748 effect in *Drosophila*. *Cell* 74:505-14.
- 749 65. Lutz M, Burke LJ, Barreto G, Goeman F, Greb H, Arnold R, Schultheiss H, Brehm A,  
750 Kouzarides T, Lobanenkova V, Renkawitz R. 2000. Transcriptional repression by the  
751 insulator protein CTCF involves histone deacetylases. *Nucleic Acids Res* 28:1707-13.
- 752 66. Testoni B, Lebosse F, Scholtes C, Berby F, Miaglia C, Subic M, Loglio A, Facchetti F,  
753 Lampertico P, Levrero M, Zoulim F. 2019. Serum hepatitis B core-related antigen  
754 (HBcrAg) correlates with covalently closed circular DNA transcriptional activity in  
755 chronic hepatitis B patients. *J Hepatol* 70:615-625.
- 756

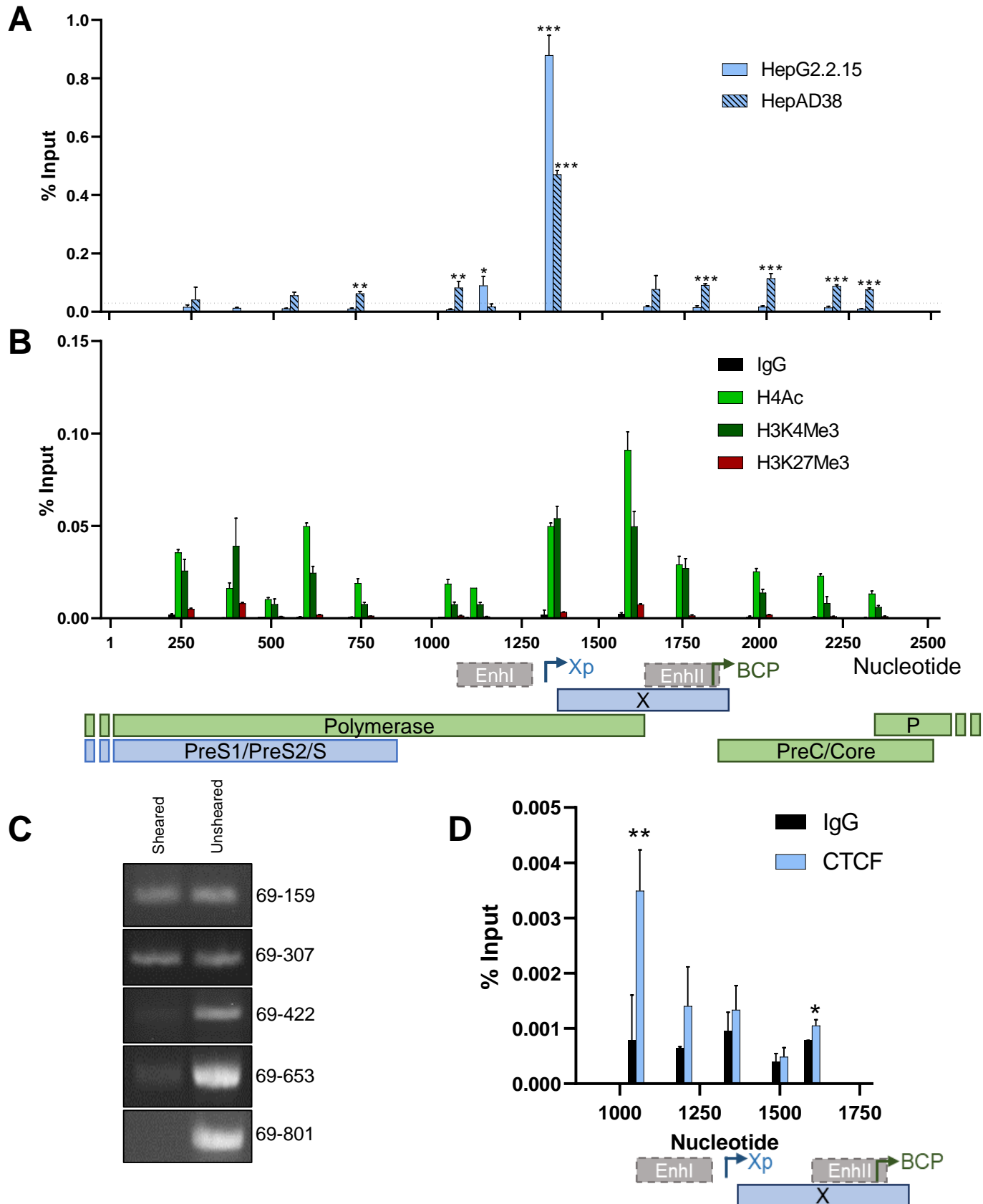


**Figure 1: CTCF associates with HBV DNA and is enriched at viral Enhancer I and X promoter.** (A) Association of CTCF with HBV DNA in HepG2.2.15 and HepAD38 cells was analysed by CHIP-qPCR and presented as % Input recovery. Statistical significance shows comparison of CTCF-specific CHIP with maximal recovery using IgG control (dotted line). (B) The distribution of histone modifications (H3K4Me3, H3K27Me3 and H4Ac) in HepG2.2.15 cells by CHIP-qPCR. (C) Efficiency of chromatin shearing in HepG2-HBV-Epi cells was assessed by PCR of sonicated versus non-sonicated chromatin. Amplicons were generated with a constant sense primer (anneals at nt 69) and anti-sense primers binding at increasing distance from the sense primer (nt 159, 307, 422, 653 and 801). Amplification of HBV DNA was assessed by SyBr green staining of bands separated by electrophoresis. (D) Association of CTCF was assessed by CHIP-qPCR. (A, B and D) Data shown are the mean  $\pm$  SEM of three technical repeats and are representative of three biological repetitions. P values were determined using a paired t test. \*denotes  $p < 0.05$ , \*\*denotes  $p < 0.01$ , \*\*\*denotes  $p < 0.001$ . Annotation of HBV genome features including open reading frames, enhancers and selected promoters is shown below the histograms.

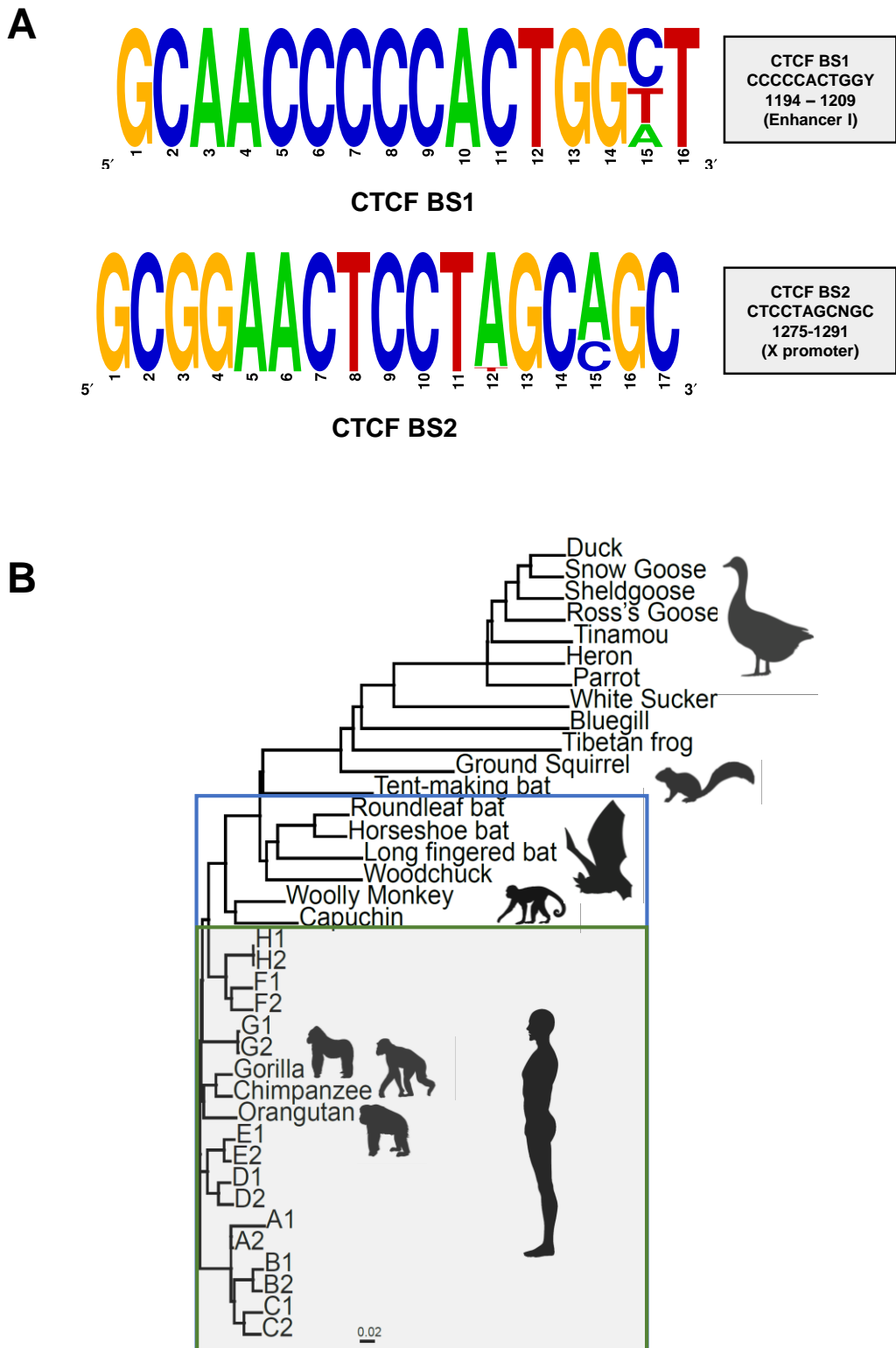


**Figure 2: Identification of conserved CTCF binding sites in HBV genomes and diverse *hepadnaviridae*.** (A) Conservation of CTCF BS among 7,313 HBV sequences (HBVdb.fr). All sites, except where indicated, are > 98% conserved. (B) Neighbor-joining phylogenetic tree of members of the *hepadnaviridae* (adapted from (1)). The green box shows viral genomes that encode both CTCF BS1 and 2 (all human and old world primate viruses), whereas the blue box shows viral genomes encoding only CTCF BS1 (new world monkeys, woodchucks and all bats except the tent making bat).

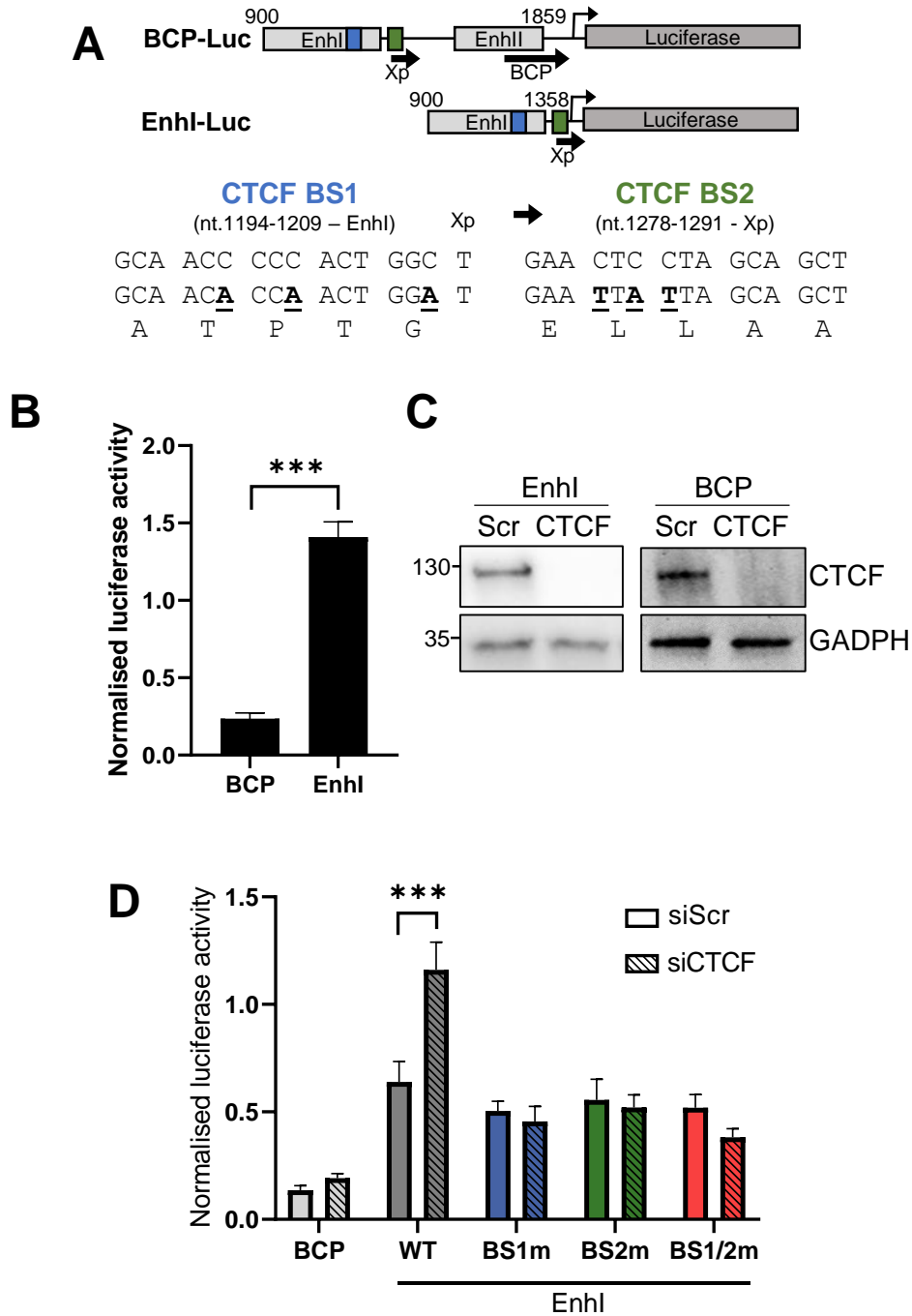


**Figure 3: CTCF represses HBV Enhancer I activity.** (A) Depiction of HBV genome regions cloned upstream of Firefly luciferase in transcriptional reporter plasmids and mutagenesis strategy of CTCF BS1 and BS2 showing viral enhancers, Xp and BCP, and CTCF BS 1 (blue) and CTCF BS 2 (green). (B) Activity of pEnhI-Luc and pBCP-Luc reporters in HepG2-NTCP cells normalized to co-transfected *Renilla* luciferase expression plasmid. (C) Western blot showing depletion of CTCF following siRNA transfection in pEnhI-Luc and pBCP-Luc transfected HepG2-NTCP cells. (D) Firefly luciferase activity normalized to *Renilla* Luciferase expression in HepG2-NTCP cells co-transfected with pGL3-basic, pEnhI-Luc or pBCP-Luc and either scrambled (Scr) or CTCF-specific siRNA duplexes. (E) Normalized luciferase activity in HepG2-NTCP cells transfected pEnhI-Luc containing mutations in CTCF binding site 1 (BS1m) or 2 (BS2m) or a combination of both (BS1/2m). Data shown are the mean +/- SEM of three independent repetitions. P values were determined by the Sidak's ANOVA multiple comparisons test. \*\*\*denotes  $p < 0.001$ .

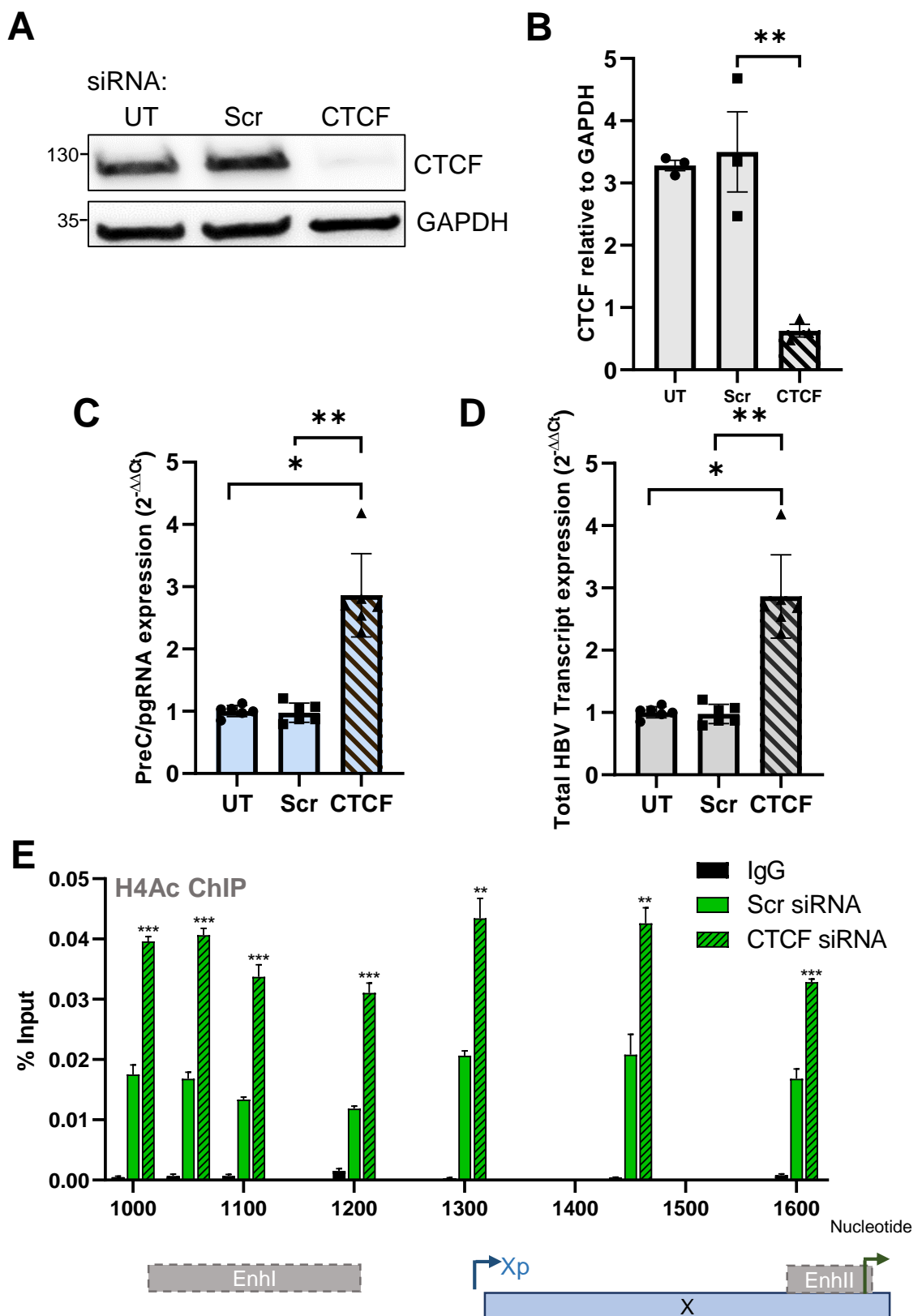


**Figure 4: CTCF represses preC/pgRNA transcription from HBV cccDNA.** HepG2-HBV-Epi cells were untransfected (UT) or transfected with scrambled (Scr) or CTCF-specific siRNA duplexes and incubated for 72 h. (A) CTCF depletion was assessed by western blotting and quantification in three independent experiments shown (B). (C, D) preC/pgRNA and total HBV RNA abundance were analysed by 4T-qPCR as previously described (46). Data are the mean  $\pm$  SD of two independent experiments performed in triplicate. Data are the mean  $\pm$  SEM of two independent experiments performed in triplicate. P values were determined by the Kruskal–Wallis ANOVA multiple group comparison. (E) Enrichment of H4Ac marks was assessed by ChIP-qPCR and shown as % Input recovery. P values were determined using a paired t test. \*denotes  $p < 0.05$ , \*\*denotes  $p < 0.01$ , \*\*\*denotes  $p < 0.001$ .

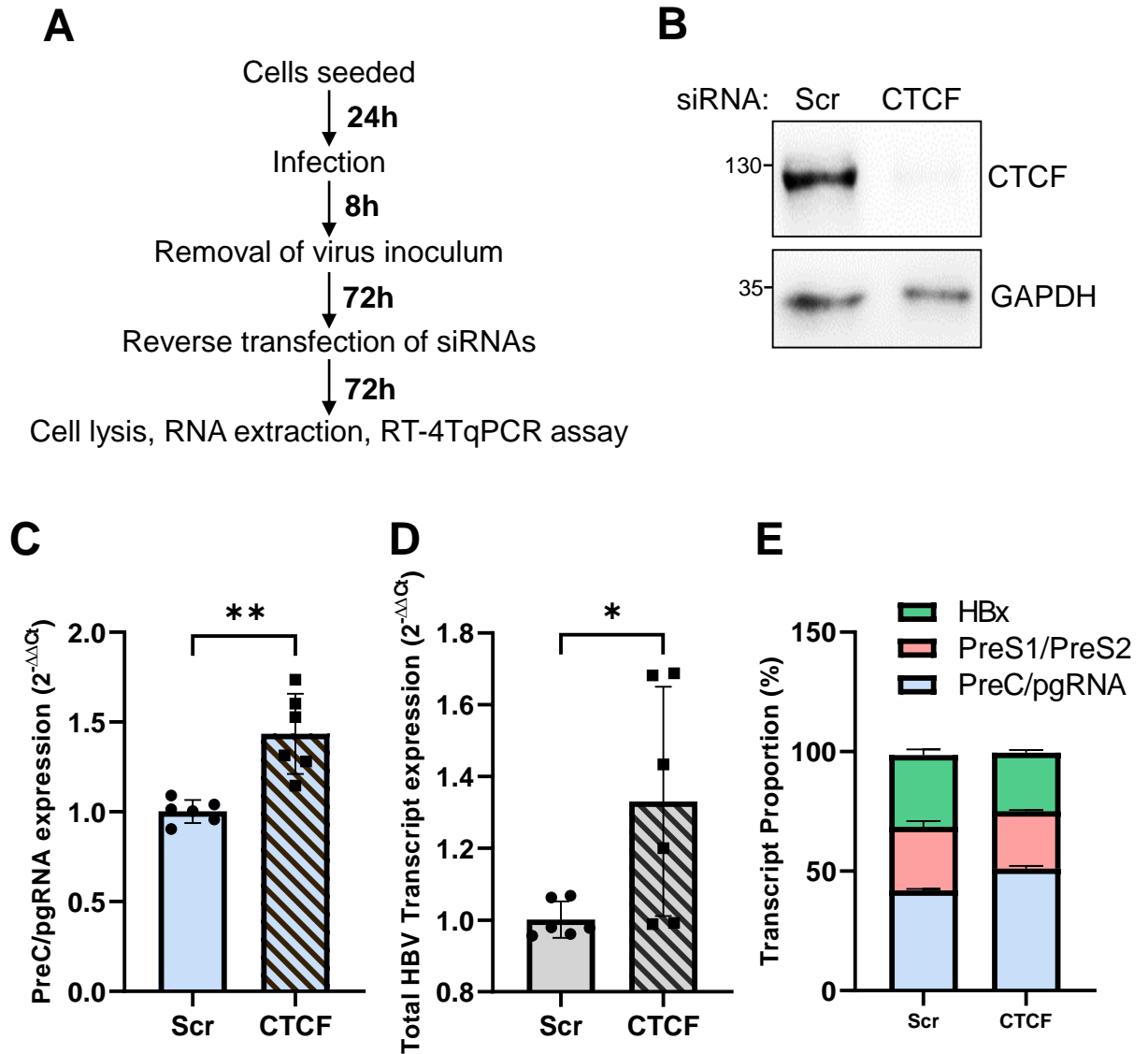
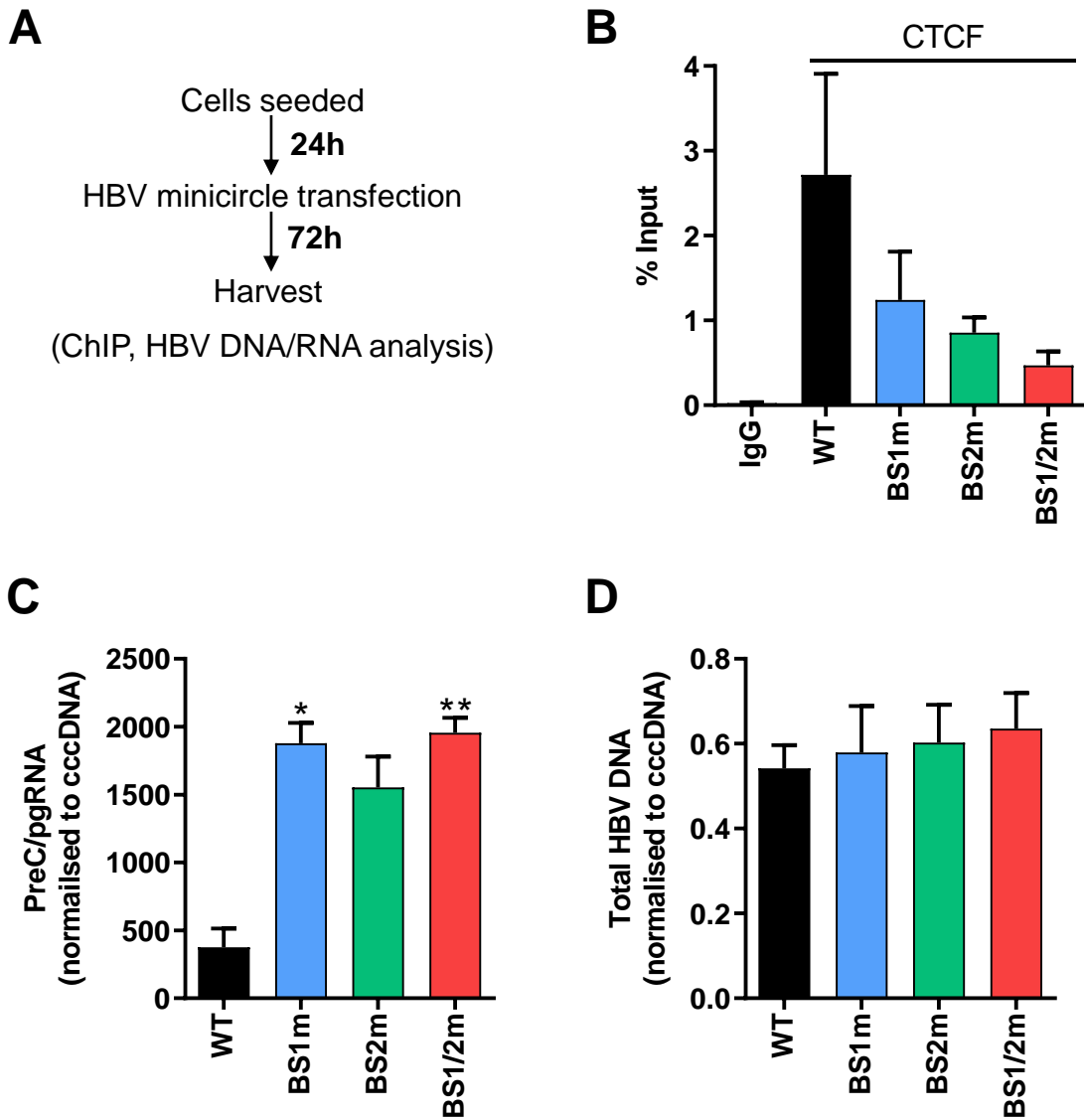
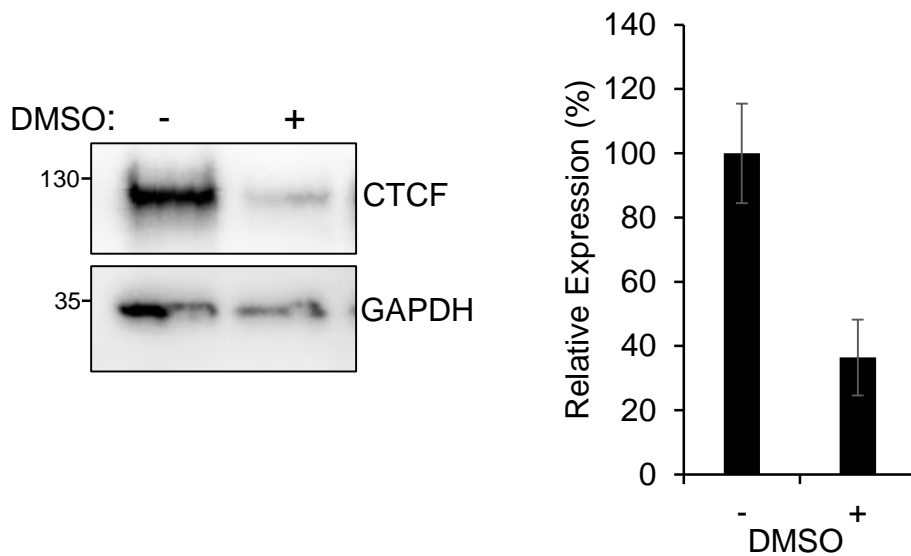


Figure 5: CTCTF represses HBV preC/pgRNA transcription in *de novo* infected HepG2-NTCP cells. (A) HBV infected HepG2-NTCP were transfected with scrambled (Scr) or CTCTF-specific siRNA duplexes and cultured for 72 h. (B) CTCTF depletion was assessed by western blotting and (C) viral transcript abundance analysed by q4T-PCR as previously described (46). Data are the mean +/- SD of two independent experiments performed in triplicate. P values were determined using the Mann-Whitney test (two group comparisons). \*denotes  $p < 0.05$ , \*\*denotes  $p < 0.01$ .

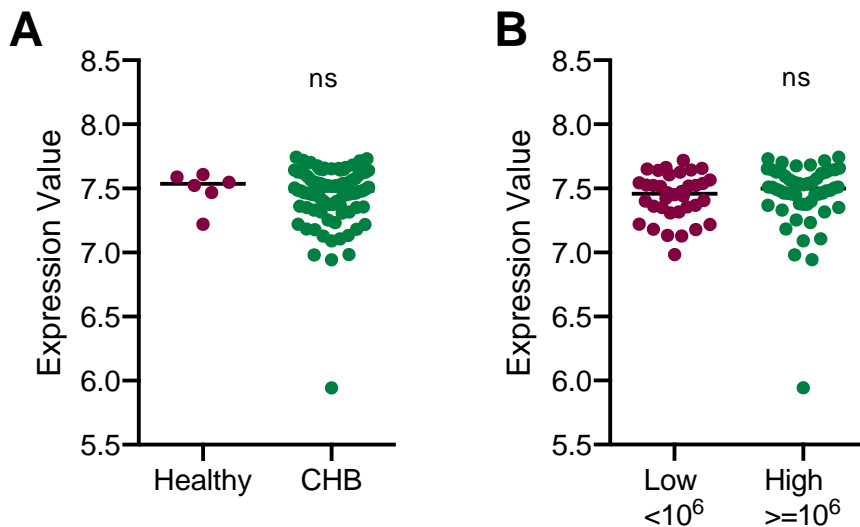


**Figure 6: Mutation of CTCF binding sites in HBV mcDNA results in increased preC/pgRNA levels.** (A) HepG2-NTCP cells were transfected with wild type HBV mcDNA (WT) or mcDNA with CTCF binding 1 (BS1m) or 2 (BS2m) or both sites mutated in combination (BS1/2m). (B) Cells were harvested 72 h post transfection and CTCF binding analysed by ChIP-qPCR and presented as % of enrichment relative to input chromatin. preC/pgRNA (C) and total HBV DNA (D) levels were quantified by qRT-PCR and normalized to cccDNA amount per cell to account for mcHBV transfection efficiency. Data are the mean +/- SEM of at least three independent experiments. P values were determined using the Kruskal–Wallis ANOVA multiple group comparison. \*denotes  $p < 0.05$ , \*\*denotes  $p < 0.01$ .





**Supplementary figure 1.** CTCF levels are reduced in DMSO treated HepG2 cells. (A) HepG2-NTCP cells were cultured with (+) or without (-) 2.5 %DMSO for 72 h. CTCF protein levels were assessed by western blotting alongside GAPDH loading control. (B) The relative expression of CTCF compared to GAPDH was quantified by densitometry. Data are the mean +/- SD of three independent experiments.



**Supplementary figure 2: CTCF expression levels in chronic hepatitis B.** (A) CTCF RNA levels were determined by high density Affymetrix microarray from liver biopsy samples in non-cirrhotic HBV infected patients (61). Patients with detectable peripheral HBV DNA (n=90) were compared against healthy patient samples (n=6). Statistical analysis was carried out using Mann-Whitney U test. (B) HBV infected patients were categorised into 2 groups based on low (n=36) or high (n=54) peripheral HBV DNA levels, and CTCF expression was compared between the two groups. Statistical analysis was carried out using the Mann-Whitney U test.